Author Manuscript

Author Manuscript

Author Manuscript

Author Manuscript

HHS Public Access

Author manuscript

Toxicol Appl Pharmacol. Author manuscript; available in PMC 2016 April 01.

Published in final edited form as:

Toxicol Appl Pharmacol. 2015 April 1; 284(1): 92–99. doi:10.1016/j.taap.2015.02.003.

Blackberry extract inhibits UVB-induced oxidative damage and inflammation through MAP kinases and NF-κB signalling pathways in SKH-1 mice skin

Sasidharan Padmaja Divya[#a,b], **Xin Wang**[#a,b], **Poyil Pratheeshkumar**[#a,b], **Young-Ok Son**[a,b], **Ram Vinod Roy**[a,b], **Donghern Kim**[b], **Jin Dai**[b], **John Andrew Hitron**[a,b], **Lei Wang**[a,b], **Padmaja Asha**[d], **Xianglin Shi**[a,b], and **Zhuo Zhang**[b,*]

[a]Center for Research on Environmental Disease, University of Kentucky, 1095 VA Drive, Lexington, KY 40536, USA.

[b]Department of Toxicology and Cancer Biology, University of Kentucky, 1095 VA Drive, Lexington, KY 40536, USA.

[d]National Centre for Aquatic Animal Health, Cochin University of Science and Technology, Cochin, India.

[#] These authors contributed equally to this work.

Abstract

Extensive exposure of solar ultraviolet-B (UVB) radiation to skin induces oxidative stress and inflammation that play a crucial role in the induction of skin cancer. Photochemoprevention with natural products represents a simple but very effective strategy for the management of cutaneous neoplasia. In this study, we investigated whether blackberry extract (BBE) reduces chronic inflammatory responses induced by UVB irradiation in SKH-1 hairless mice skin. Mice were exposed to UVB radiation (100 mJ/cm^2) on alternate days for 10 weeks, and BBE (10% and 20%) was applied topically a day before UVB exposure. Our results show that BBE **suppressed** UVB-induced hyperplasia and reduced infiltration of inflammatory cells in the SKH-1 hairless mice skin. BBE treatment reduced glutathione (GSH) depletion, lipid peroxidation (LPO), and myeloperoxidase (MPO) in mouse skin by chronic UVB exposure. BBE significantly decreased the level of pro-inflammatory cytokines IL-6 and TNF-α in UVB-exposed skin. Likewise, UVB-induced inflammatory responses were diminished by BBE as observed by a remarkable reduction in the levels of phosphorylated MAP Kinases, Erk1/2, p38, JNK1/2 and MKK4. Furthermore, BBE also reduced inflammatory mediators such as cyclooxygenase-2 (COX-2), prostaglandin E_2 (PGE_2), and inducible nitric oxide synthase (iNOS) levels in UVB-exposed skin. Treatment with

© 2015 Published by Elsevier Inc.

[*] To whom correspondence should be addressed at Department of Toxicology and Cancer Biology, University of Kentucky, 1095 Veterans Drive, Lexington, Kentucky 40536, USA. zhuo.zhang@uky.edu; Tel: (859) 323 9591; Fax: (859)323 1059..

Publisher's Disclaimer: This is a PDF file of an unedited manuscript that has been accepted for publication. As a service to our customers we are providing this early version of the manuscript. The manuscript will undergo copyediting, typesetting, and review of the resulting proof before it is published in its final citable form. Please note that during the production process errors may be discovered which could affect the content, and all legal disclaimers that apply to the journal pertain.

Conflict of interest

The authors declare that there is no conflict interest.

Author Manuscript Author Manuscript Author Manuscript Author Manuscript

BBE inhibited UVB-induced nuclear translocation of NF-κB and degradation of IκBα in mouse skin. **Immunohistochemistry** analysis revealed that topical application of BBE inhibited the expression of 8-oxo-7, 8-dihydro-2'-deoxyguanosine (**8-oxodG**), cyclobutane pyrimidine dimers (CPD), proliferating cell nuclear antigen (PCNA), and cyclin D1 in UVB-exposed skin. Collectively, these data indicates that BBE protects from UVB-induced oxidative damage and inflammation by modulating MAP kinase and NF-κB signaling pathways.

Keywords

Blackberry extract; Ultraviolet radiation; Inflammation; COX-2; NF-κB

Introduction[1]

Ultraviolet B light has been recognized as a complete carcinogen, responsible for both initiation and promotion of skin carcinogenesis (Ananthaswamy and Pierceall 1990). At least 50% of UVB-induced skin damage is attributable to the formation of reactive oxygen species (ROS). In addition to the generation of ROS, UVB irradiation also induces acute skin inflammation (Sano and Park 2014). Increased ROS modulates the inflammatory responses through activation of mitogen-activated protein kinases (MAPK), a factor known to contribute to skin carcinogenesis (Sharma et al. 2007). UVB induces constitutive expression of COX-2, which is the primary source of elevated PGE_2 in the skin (Burns et al. 2013).

NF-κB is another major factor mediating UVB-induced inflammatory responses through the expression of various proinflammatory proteins such as iNOS, TNF-α, and IL-6 (Choi et al. 2014; Sharma and Katiyar 2010). UVB also indirectly damages DNA by increasing levels of ROS which facilitate oxidative damage to DNA bases, such as formation of 8-oxo-7, 8-dihydro-2'-deoxyguanosine (**8-oxodG**) (de Gruijl 2002). In addition, UVB-induced DNA damage in the form of cyclobutane pyrimidine dimers (CPDs) has also been implicated in skin cancer risk (Vaid et al. 2010).

The dietary consumption of whole fruits containing antioxidants could quench ROS, which has been implicated in carcinogenesis (Feng et al. 2004). Blackberries rank among the highest of all natural foods in anthocyanins (Halvorsen et al. 2006), and display potent antioxidant and anti-cancer properties (Murapa et al. 2012; Seeram et al. 2006). Six distinct anthocyanins were identified in BBE and cyanidin-3-glucoside (C3G) is one of them (Murapa et al. 2012). We have recently shown that C3G inhibits UVB-induced oxidative stress and inflammation in SKH-1 hairless mouse skin (Pratheeshkumar et al. 2014).

In this study, we investigated the protective effect of BBE on UVB-induced inflammation and early biomarkers associated with photocarcinogenesis using the SKH-1 hairless mouse

[1]ADPH: 10-acetyl-3,7-dihydroxyphenoxazine; BBE: blackberry extract; C3G: cyanidin-3-glucoside; COX-2: cyclooxygenase-2; CPD: cyclobutane pyrimidine dimers; **8-oxodG**: 8-dihydro-2'-deoxyguanosine; EDTA: ethylenediaminetetraacetic acid; GSH: glutathione; iNOS: inducible nitric oxide synthase; IL-6: interleukin-6; LPO: lipid peroxidation; MPO: myeloperoxidase; PGE2: prostaglandin E_2; ROS: reactive oxygen species; TBARS: thiobarbituric acid reactive substances; TNFα: tumor necrosis factor-α; UVB: ultraviolet B

Author Manuscript Author Manuscript Author Manuscript Author Manuscript

skin model. We found that topical application of BBE to SKH-1 hairless mice prior to UVB radiation resulted in a significant reduction of UVB-induced (i) skin edema, hyperplasia, and leukocyte infiltration; (ii) COX-2, iNOS and PGE_2 production; (iii) proinflammatory cytokine levels (TNF-α and IL-6); (iv) cell proliferation protein markers (PCNA and cyclin D1); (v) protein expression of phosphorylated of ERK1/2, JNK1/2, p38 and MKK4; (vi) oxidative stress and formation of **8-oxodG** and CPDs; and (vii) activation of NF-κB and IKKα, and degradation of IκBα.

Materials and methods

Animals

Female SKH-1 hairless mice (6-8 weeks old) were purchased from Charles River Laboratory (Wilmington, MA). The mice were acclimatized for at least 1 week before experimental use in the animal resource facility and maintained under standard conditions of a 12 h dark/12 h light cycle at a temperature of 24±2°C and relative humidity of 50±10%. The Institutional Animal Care and Use Committee of the University of Kentucky at Lexington approved the animal protocol used in this study.

Antibodies and assay kits

Antibodies specific for p-p38, p38, p-MKK4, MKK4, and iNOS were obtained from Cell Signaling Technology (Beverly, MA). The antibodies specific for PCNA, p-ERK, ERK, p-JNK, JNK, NF-κB/p65, IKKα, IκBα, COX-2, TNF-α, cyclin D1, β-actin and the secondary antibody were from Santa Cruz Biotechnology, Inc. (Santa Cruz, CA). Anti-cyclobutane pyrimidine dimer antibody was from Kamiya Biomedical Co., (Seattle, WA) and anti-TNF-α antibody for immunohistochemistry staining was from Novus Biologicals Inc, (Littleton, CO). Assay kits for MPO, GSH, and PGE_2 analysis were from Cayman Chemical (Ann Arbor, MI). The assay kit for thiobarbituric acid reactive substances (TBARS) was purchased from BioAssay Systems (Hayward, CA, USA), and the NF-κB/p65 Trans™ ELISA kit was from Active Motif, (Carlsbad, CA). Enzyme-linked immunosorbent assay kits specific for mouse TNF-α and IL-6 were from PromoKine (Heidelberg, Germany). For the Western blots, nuclear and cytoplasmic extraction kits as well as the Coomassie protein analysis reagents were from Thermo (Rockford, IL). The horseradish peroxidase conjugated antibody used for Western blots was from Pierce (Rockford IL).

Preparation of blackberry extract—Fresh blackberries obtained from Kroger, Inc., during the harvest season, were washed with a mild detergent and rinsed three times with Milli-Q deionized water to remove possible pesticide and preservative residues. Blackberry extract was prepared using the protocol described previously (Feng et al. 2004) and was diluted in acetone for topical application. We had performed some pilot pharmacological studies both in vitro and in vivo with difference concentrations of blackberry extract. The concentration of 10% and 20% were found to be more effective.

UVB light source and irradiation protocol

SKH-1 hairless mice were randomly divided into 6 groups with 12 mice/group. Mice were exposed to UV radiation from a band of four FS24T1 UVB lamps (Daavlin, UVA/ UVB

Author Manuscript Author Manuscript Author Manuscript Author Manuscript

Research Irradiation Unit, Bryan, OH) equipped with an electronic controller to regulate UV dosage, at a distance of 23 cm between the light source and the target skin. Topical treatments to mouse dorsal skin include either acetone (control group, 50 μL/mouse) or BBE (10% and 20% in acetone) the day before UV exposure to avoid possible sunscreen effect. Murine skin exposure was 100 mJ/cm^2 of UVB, 3 times per week for 10 weeks. After 10 weeks of exposure ± BBE treatment, animals were euthanized at either 2 h or 24 h after the last UVB irradiation, and dorsal skin tissues were excised and processed as indicated.

Quantitation of PGE_2

PGE_2 levels in skin samples were determined using the protocol provided by the kit's manufacturer. Briefly, skin samples were homogenized in 100 mM phosphate buffer, pH 7.4 containing 1 mM ethylenediaminetetraacetic acid (EDTA) and 10 μM indomethacin using a polytron homogenizer (Fisher Scientific, GA). Supernatants were collected and analyzed for PGE_2 concentration.

Tissue glutathione assay

Mouse skin tissue was homogenized in cold buffer (50 mM Phosphate, pH 6-7, containing 1 mM EDTA), and centrifuged at 10,000 ×g for 15 min at 4 °C. Total GSH content in the supernatants was determined using the assay protocol provided by the kit's manufacturer.

TBARS assay

Skin tissue was homogenized by sonication in ice cold PBS. After centrifugation at 12,000 ×g for 15 min at 4°C, lipid peroxidation was assessed in the supernatant using the protocol provided by the kit's manufacturer. Reacted samples added to wells of a 96 well plate were measured spectrophotometrically at 532 nm using malondialdehyde (MDA) as a standard.

MPO assay

Tissue myeloperoxidase was measured according to the protocol provided by the kit's manufacturer. This assay provides a fluorescence-based method for detecting the MPO activity in tissue lysates. The assay utilizes the peroxidase component of MPO, and the reaction between H_2O_2 and 10-acetyl-3,7-dihydroxyphenoxazine (ADHP) produces the fluorescent compound resorufin.

Assay for proinflammatory cytokines

TNF-α and IL-6 levels were assessed using epidermal homogenates from each treatment group. Cytokine levels were assessed using the protocol provided by the kit's manufacturer.

ELISA for NF-KB/p65

Quantitative analyses of NF-κB/p65 levels were assessed using the protocol provided by the kit's manufacturer. Nuclear extracts of epidermal skin samples from various treatment groups were prepared using the Nuclear Extraction Kit (Active Motif) according to the manufacturer's directions. Recorded absorbance was at 450 nm with reference taken at 650 nm. The assay was performed in duplicate and the results are expressed as the percentage of the control (non-UVB exposed) absorbance.

Author Manuscript Author Manuscript Author Manuscript Author Manuscript

Histopathological analysis

Skin samples from mice were fixed in 10% neutral buffered formalin, paraffin embedded, and 4-6 μm thick sections were stained with hemotoxylin and eosin (H&E) to permit morphologic evaluation by light microscopy.

Immunoblotting analysis

Epidermis from the whole skin was isolated and homogenized in ice-cold RIPA buffer (Sigma-Aldrich) with freshly added protease inhibitor cocktail. The homogenate was centrifuged at 14 000 xg for 25 min at 4°C and the supernatant (total cell lysate) was collected, aliquoted and stored at −80°C. Nuclear and cytoplasmic extracts were prepared according to the manufacturer's protocol. The protein concentration was determined using the Coomassie method. Approximately 40 μg cellular proteins, applied to a 6%–12% SDS-polyacrylamide gel and separated electrophoretically, were transferred to a nitrocellulose membrane. Membranes were blocked with 5% fat-free dry milk in 1X Tris-buffered saline (TBS) and incubated with antibodies, as indicated. Membrane incubation with horseradish peroxidase-conjugated antibodies followed, and enhanced chemiluminescence reagent permitted visualization of the proteins (Perkin Elmer, Boston, MA). To verify equal protein loading on the gel, blots were stripped, and re-probed for β-actin.

RNA extraction and quantitative Real-Time PCR

TRIzol reagent (Invitrogen, CA) extracted total RNA from mouse epidermis using the protocol recommended by the manufacturer. The mRNA expression of PCNA and cyclin D1 in skin samples was determined using real-time quantitative PCR with a Bio-Rad MyiQ thermocycler and SYBR green detection system (Bio-Rad, CA), as described previously (Ding et al. 2013; Pratheeshkumar et al. 2014).

Immunohistochemistry analysis—Skin samples embedded in optimal cutting temperature medium (OCT) were immediately transferred to liquid nitrogen (−80°C) for storage. Frozen skin sections (5 μm thick) were fixed (4% paraformaldehyde), blocked (5% horse serum), and incubated with various antibodies for 2 h at room temperature : anti-COX-2 (1:100); anti-Cyclobutane pyrimidine dimer (1:100); anti-p65 (1:100); **anti-8-oxodG** (1:50); anti-TNF-α (1:200); anti-PCNA (1:100); or anti-cyclin D1 (1:50). Washed tissue sections were incubated with biotinylated secondary antibody for 45 min according to the Vectastain ABC Kit protocol (Vector Laboratories, Burlingame, CA). After additional washing with PBS, DAB solution provided visualization of antibody binding, and hematoxylin used as a counterstain.

Statistical analysis

Expressed data are the mean ± standard deviation (SD). Statistically significant differences among treatment groups were determined by One-way analysis of variance (ANOVA). A p-value of <0.05 was considered as statistically significant.

Author Manuscript Author Manuscript Author Manuscript Author Manuscript

Results

BBE inhibits cutaneous edema, hyperplasia and leukocyte infiltration in SKH-1 mouse skin caused by repeated UVB exposure

UVB irradiation leads to cutaneous edema, hyperplasia, erythema, leukocyte infiltration, dilation of dermal blood vessels and vascular hyperpermeability (Sharma and Katiyar 2010). In the present study, we assessed the effect of BBE on skin edema in UVB exposed SKH-1 hairless mice. Exposure of mouse skin to UVB radiation resulted in a significant increase in bifold-skin thickness compared to non-irradiated skin, while BBE treatment alone did not cause any change in skin thickness (Fig. 1A). H&E staining revealed that UVB irradiation caused hyperplasia, and a mixed cell infiltration in the dermis (Fig. 1B). As expected, leukocyte infiltration and epidermal hyperplasia induced by UVB irradiation were reduced by topical administration of BBE. Repeated UVB exposure resulted in a 2.0-fold increase in myeloperoxidase activity in the irradiated skin compared with skin without UVB irradiation. BBE treatment significantly ($p < 0.05$) decreased MPO activity (Fig. 1C).

BBE inhibits oxidative stress and DNA damage in SKH-1 mouse skin caused by repeated UVB exposure

UVB irradiation generates excessive ROS and causes oxidative DNA damage, resulting in oxidative stress. Many studies suggest that topical application of antioxidants can provide a photoprotective effect and might be an effective strategy for reducing UV irradiation-induced oxidative damage to the skin (Hsieh et al. 2005; C-W Lee et al. 2013; Sumiyoshi and Kimura 2009). LPO induced by ROS is considered one of the major manifestations of oxidative stress (Khan et al. 2012). In the present study, we assessed the effect of topical administration of BBE on repeated UV exposure to mouse skin by measuring the concentration of the short-chain aldehyde, MDA, which is the by-product of LPO. Our results demonstrate that treatment with BBE effectively inhibits the UVB-mediated increase of epidermal MDA when compared with UVB exposure alone (Fig. 2A). In a similar manner, the effect of multiple UVB irradiation exposures on GSH levels was determined. Topical treatment of mouse skin with BBE reduced GSH depletion, maintaining a level similar to the non-irradiated control group (Fig. 2B). BBE treatment alone did not alter glutathione level which was similar to that in unexposed controls.

UVB also causes direct DNA damage by oxidation of nucleotides and produces 8-OHdG (Afaq et al. 2007). Employing **immunohistochemistry** analysis, we assessed the effect of topical application of BBE on UVB-mediated DNA damage to mouse epidermis. UVB irradiation to SKH-1 hairless mouse skin increased 8-oxodG formation when compared to non-irradiated control skin (Fig. 2C). In skin samples obtained 24 h after UVB exposure, the number of 8-oxodG positive cells were significantly higher when compared to the non-irradiated control tissue, but topical BBE treatment markedly reduced 8-oxodG formation induced by UVB when compared to the UVB-irradiated group. CPD represents the major form of UVB-induced damage to DNA. Therefore, CPD formation was determined to evaluate the protective effect of BBE. UVB irradiation to SKH-1 hairless mouse skin strongly increased CPD formation. This effect was markedly suppressed by the topical treatment of BBE (Fig. 2D).

Author Manuscript Author Manuscript Author Manuscript Author Manuscript

BBE inhibits inflammation irradiated by repeated UVB exposure in SKH-1 mouse skin

Previous studies have demonstrated that the expressions of proinflammatory enzymes (iNOS and COX-2) and cytokines (TNF-α and IL-6) are induced by UVB exposure (Afaq et al. 2003b; JA Lee et al. 2013; Sharma and Katiyar 2010). We examined the effect of BBE on UVB-induced expressions of epidermal iNOS, COX-2, and TNF-α protein. Immunoblotting analysis revealed that UVB exposure to SKH-1 hairless mice resulted in a marked increase in expressions of epidermal iNOS, COX-2, and TNF-α compared to the non-irradiated control group. However, topical application of BBE significantly reduced the expressions of iNOS, COX-2, and TNF-α when compared to skin exposed to UVB irradiation alone. In addition, topical application of BBE alone did not produce any change in expressions of epidermal iNOS, COX-2, or TNF-α when compared to skin from non-irradiated control animals (Fig. 3A). **Immunohistochemistry** analysis of COX-2 and TNF-α produced essentially the same results (Fig. 3B). PGE_2 levels were also determined in these samples. As shown in Fig. 3C, the levels of PGE_2 in UVB-exposed mouse skin were significantly higher ($p<0.05$) than in the non-UVB-exposed mouse skin samples. Topical treatment of BBE significantly inhibited ($p<0.05$) UVB-induced elevation in the levels of PGE_2 in the mouse skin. Similarly, the levels of both proinflammatory cytokines, TNF-α (Fig. 3D) and IL-6 (Fig. 3E) in BBE treated group were also significantly ($p<0.05$) reduced when compared with irradiated tissue that was not treated.

BBE inhibits phosphorylation of MAPK proteins in SKH-1 mouse skin caused by repeated UVB exposure

Previous studies have demonstrated that UVB-induced oxidative stress is important in the activation of MAPK and that this activation plays an important role in the promotion of photocarcinogenesis (Afaq et al. 2003a; Vayalil et al. 2003). Therefore, we assessed the effect of topical administration of BBE on SKH-1 hairless mouse skin on activation of MAPK family proteins (ERK1/2, p38, JNK1/2 and MKK4) after repeated UVB exposures by Western blot analysis. Our results indicate that multiple UVB exposures to mouse skin resulted in an increased phosphorylation of ERK1/2, p38, JNK1/2 and MKK4 proteins of MAPK family. As shown in Fig. 4, Western blot analysis revealed that BBE markedly reduced UVB-mediated phosphorylation of ERK1/2, p38, JNK1/2 and MKK4 proteins as compared to UVB exposure alone, and treatment with BBE alone did not induce phosphorylation of ERK1/2, p38, JNK1/2 and MKK4 proteins. Furthermore, the total amount of ERK1/2, JNK, and p38 proteins remained unchanged in each treatment group.

BBE inhibits activation of NF-κB pathway in SKH-1 mouse skin induced by repeated UVB exposure

NF-κB/p65 is a downstream target of the MAPK signal transduction pathway (**Sharma, S.D., Meeran, S.M., Katiyar, S.K., 2007**). Our Western blot analysis indicated that repeated exposure of mouse skin to UVB stimulated the phosphorylation of NF-κB/p65 as compared to the non–UVB-exposed control mouse skin. Topical application of BBE markedly reduced the UVB-induced NF-κB phosphorylation in a dose-dependent manner (Fig. 5A). **Immunohistochemistry** analysis confirmed these results (Fig. 5B). Moreover, BBE also inhibited the translocation of NF-κB/p65 to the nucleus compared with UVB-

Author Manuscript Author Manuscript Author Manuscript Author Manuscript

exposed skin alone (Fig. 5C). Previous studies have shown that exposure to UVB radiation resulted in degradation of the IκBα protein with subsequent activation and translocation of NF-κB/p65 to the nucleus (Mantena and Katiyar 2006; Pratheeshkumar et al. 2014b). This mechanism involves phosphorylation of serine residues in IκBα by IKK, leading to degradation of IκBα and activation of NF-κB. Repeated UVB exposure triggers activation of IKKα, which is essential for the degradation of IκBα. To study the inhibitory effect of BBE on UVB-induced degradation of IκBα, we investigated the cytoplasmic level of IκBα protein expression. Western blot analysis demonstrated that topical application of BBE inhibited UVB-mediated degradation of IκBα (Fig. 5D). These studies also indicated that the levels of activated IKKα were higher in the mouse skin irradiated by UVB; however, topical application of BBE inhibited the levels of activated IKKα in cytosols (Fig. 5D). The inhibitory effect of BBE on UVB-induced NF-κB activation was confirmed using ELISA for NF-κB/p65 (Fig. 5E).

BBE inhibits cyclin D1 and PCNA levels induced by repeated UVB exposure in SKH-1 mouse skin

Photocarcinogenesis is often associated with enhanced expression of the cell cycle regulatory protein, cyclin-D1 and the cell proliferation marker, PCNA. Western blot analysis showed that UVB exposure increased cyclin D1 and PCNA protein expression in irradiated skin when compared to non-UVB-exposed mouse skin. Topical application of BBE reduced cyclin D1 and PCNA expression induced by repeated UVB exposure (Fig. 6A). **Immunohistochemistry** analysis (Fig. 6B) and mRNA expression by real-time PCR, as shown in Figs. 6C and 6D confirmed these data.

Discussion

Skin cancer is the most common form of cancer in the United States (Rogers et al. 2010). Each year there are more newly diagnosed cases of skin cancer than the combined incidence of cancers of the breast, prostate, lung, and colon (Society 2012). One among five Americans is estimated to develop skin cancer in their lifetime (Robinson 2005). The major agent causing skin cancer is UV radiation from sunlight (Sarasin 1999); chronic exposure to UV radiation leads to skin cancer (Koh 1995). Given the increasing morbidity, incidence, and cost of this disease, research has focused on seeking novel chemopreventive agents that will inhibit non-melanoma skin cancer formation and progression (Phillips et al. 2013). Investigations using animal models and epidemiological studies indicate that dietary consumption of phytochemicals might reduce the incidence of cancers and other chronic diseases (Feng et al. 2004; Pratheeshkumar et al. 2012). Among the potential chemoprotective diets, growing attention has been dedicated to berry products, such as blackberry, strawberry, cranberry, black raspberry, and blueberry (Feng et al. 2004). Electron spin resonance studies suggest that blackberry extract is a potent scavenger of free radicals, including .OH and O_2.- radicals (Feng et al. 2004). Prevention of human chronic diseases, including cancer, may occur with scavenging of ROS and reduction of oxidative stress. In this study, we examined the ability of BBE to protect skin from UVB-induced damage.

Author Manuscript Author Manuscript Author Manuscript Author Manuscript

Skin exposure to UVB radiation depletes antioxidant defensive capabilities at irradiated sites. ROS plays a significant role in UVB-induced skin carcinogenesis (Agar et al. 2004; Merwald et al. 2005). In the body, endogenous antioxidants offset UV-induced oxidative stress by neutralization of the ROS before oxidative changes occur in the tissues. GSH, a free radical-scavenger as well as a cofactor for protective enzymes, plays a pivotal role in protecting cells against oxidative damage. UVB irradiation leads to decreased levels of GSH due to leakage and oxidation of GSH (Merwald et al. 2005). In this study, we examined the effect of BBE on antioxidant status in mouse skin under chronic UVB irradiation. Chronic UVB exposure to mouse skin significantly reduced GSH content; and topical application of BBE dramatically offset this reduction.

UVB-induced oxidation of lipids is another important source of oxidative stress. Lipid peroxidation is significantly increased in UVB-exposed mouse skin (Pratheeshkumar et al. 2014a). Direct absorption of UVB by DNA causes formation of thymine dimers in DNA bases (Heck et al. 2003). In addition, electron transfer or singlet molecular oxygen produced by UVB radiation targets guanine, giving rise to 8-hydroxy-2-deoxyguanosine (8-OHdG) in DNA strands (Cadet et al. 1999). This molecule is a well-known biomarker of oxidative stress, and the major mutagenic form of oxidative DNA damage. Our results demonstrate that BBE offers SKH-1 mouse skin protection against UVB-induced oxidation of lipids and oxidative DNA damage. These findings are similar to those obtained by the topical application of quercitrin or C3G to mouse skin (Pratheeshkumar et al. 2014b; Yin et al. 2013).

COX-2 plays a key role in UVB-induced inflammation by catalysing the generation of PGE_2 from prostanoid precursors (Fischer et al. 2007). Overexpression of COX-2 has been demonstrated in several animal models of inflammation and tumors (Pratheeshkumar and Kuttan 2010; P Pratheeshkumar and Girija Kuttan 2011). Therefore, the inhibition of COX-2 expression should impede the development of skin cancer. Nitric oxide (NO) is thought to be an important mediator of inflammation, and overexpression of iNOS is detected in several human tumors (Cherng et al. 2011; Chiang et al. 2005; Gallo et al. 1998). Previous studies indicate a link between iNOS and COX-2 expression (Cherng et al. 2011; Yoshida et al. 2006). Consistent with this report, our study shows increased COX-2, iNOS, and PGE_2 levels in UVB-exposed mouse skin. Our results also show that topical BBE treatment could effectively suppress them. Along with these proinflammatory mediators, proinflammatory cytokines such as TNF-α and IL-6 have been shown to be involved in UVB induced inflammation and carcinogenesis (Sharma and Katiyar 2010). Our data indicate that topical application of BBE significantly inhibited UVB-induced expression of these proinflammatory cytokines in mouse skin.

Nuclear factor (NF)-κB is a ubiquitous nuclear transcription factor responsive to diverse stimuli, such as TNF, UV radiation, interleukins, endotoxins, as well as others (Poyil Pratheeshkumar and Girija Kuttan 2011). Aberrant, sustained activation of NF-κB has been reported in numerous tumors and was implicated in various stages of photocarcinogenesis (Khan et al. 2012; Wang et al. 2012). In the present study, topical treatment with BBE effectively inhibited the activation and nuclear translocation of NF-κB/p65 in UVB exposed mouse skin. In addition, BBE also inhibited the UVB induced degradation of the IκBα

Author Manuscript Author Manuscript Author Manuscript Author Manuscript

protein. Collectively, our results demonstrate that topical treatment of BBE prevents UVB-induced activation and nuclear translocation of NF-κB/p65 by inhibiting the activation of IKKα and subsequent degradation of IκBα protein in mouse skin.

MAPK are made up of three family members that include extracellular-signal-related protein kinases (ERKs), c-JUN N-terminal kinases stress-activated protein kinases (JNKs/SAPs) and p38 kinases (Einspahr et al. 2008). During the activation of p38MAPK, several upstream kinases, including MAP kinase kinases (MKK) are also involved. Previous studies have shown that UVB mediated oxidative stress modulates the levels of phosphorylated MAPKs including ERK1/2, JNK, and p38, and that these phosphorylated proteins are involved in carcinogenesis (Dickinson et al. 2011; Yoon et al. 2010). Moreover, ERK and p38 proteins of MAPK family have been shown to modulate NF-κB activation (Sharma and Katiyar 2010). The present study demonstrates that BBE inhibits UVB-induced phosphorylation of ERK, p38 MAPK, JNK and MKK4 on mouse skin, thereby reducing the risk of carcinogenesis.

Chronic inflammation is linked to enhanced cell proliferation, which is the hallmark of cancer development (Gu et al. 2007). Biomarkers of cellular proliferation, such as epidermal PCNA and cyclin D1 are used to determine proliferation potential during tumorigenesis, and clinical prognosis (Sharma and Katiyar 2010; Zhaorigetu et al. 2003). In the present study, topical application of BBE to mouse skin provided a highly significant inhibition of UVB-induced epidermal thickening, and decreased mRNA and protein expressions of PCNA and cyclin D1. Similar results were observed in UVB-exposed skin by dietary GSPs (Sharma and Katiyar 2010).

In summary, the results from the present study show that topical application of BBE is able to protect mouse skin from UVB-induced oxidative damage and inflammation by modulating MAP kinase and NF-κB signaling pathways, indicating potential efficacy of BBE against UVB-induced skin damage. Further long term *in vivo* carcinogenesis study is needed to fully evaluate molecular targets of BBE against skin cancer development induced by UVB.

Acknowledgements

This research was supported by National Institutes of Health/National Institutes of Environmental Health Sciences (R01ES017244 and R21ES019249).

References

Afaq F, Adhami VM, Ahmad N. Prevention of short-term ultraviolet B radiation-mediated damages by resveratrol in SKH-1 hairless mice. Toxicol. Appl. Pharmacol. 2003a; 186:28–37. [PubMed: 12583990]

Afaq F, Adhami VM, Ahmad N, Mukhtar H. Inhibition of ultraviolet B-mediated activation of nuclear factor κB in normal human epidermal keratinocytes by green tea constituent (-)-epigallocatechin-3-gallate. Oncogene. 2003b; 22:1035–1044. [PubMed: 12592390]

Afaq F, Syed DN, Malik A, Hadi N, Sarfaraz S, Kweon MH, et al. Delphinidin, an anthocyanidin in pigmented fruits and vegetables, protects human hacat keratinocytes and mouse skin against UVB-mediated oxidative stress and apoptosis. J. Invest. Dermatol. 2007; 127:222–232. [PubMed: 16902416]

Author Manuscript Author Manuscript Author Manuscript Author Manuscript

Agar NS, Halliday GM, Barnetson RS, Ananthaswamy HN, Wheeler M, Jones AM. The basal layer in human squamous tumors harbors more UVA than UVB fingerprint mutations: A role for UVA in human skin carcinogenesis. Proc. Natl. Acad. Sci. U. S. A. 2004; 101:4954–4959. [PubMed: 15041750]

Ananthaswamy H,N, Pierceall WE. Molecular mechanisms of ultraviolet radiation carcinogenesis. Photochem. Photobiol. 1990; 52:1119–1136. [PubMed: 2087500]

Burns EM, Tober KL, Riggenbach JA, Schick JS, Lamping KN, Kusewitt DF, et al. Preventative topical diclofenac treatment differentially decreases tumor burden in male and female SKH-1 mice in a model of UVB-induced cutaneous squamous cell carcinoma. Carcinogenesis. 2013; 34:370–377. [PubMed: 23125227]

Cadet J, Douki T, Pouget JP, Ravanat JL. Singlet oxygen DNA damage products: Formation and measurement. Methods in Enzymol. 1999; 319:143–153. [PubMed: 10907507]

Cherng JM, Tsai KD, Perng DS, Wang JS, Wei CC, Lin JC. Diallyl sulfide protects against ultraviolet B-induced skin cancers in SKH-1 hairless mouse: Analysis of early molecular events in carcinogenesis. Photoderm. Photoimmunol. Photomed. 2011; 27:138–146.

Chiang YM, Lo CP, Chen YP, Wang SY, Yang NS, Kuo YH, et al. Ethyl caffeate suppresses NF-κB activation and its downstream inflammatory mediators, iNOS, COX-2, and PGE-2 in vitro or in mouse skin. Br. J. Pharmacol. 2005; 146:352–363. [PubMed: 16041399]

Choi YJ, Uehara Y, Park JY, Kim SJ, Kim SR, Lee HW, et al. Mhy884, a newly synthesized tyrosinase inhibitor, suppresses UVB-induced activation of NF-κB signaling pathway through the downregulation of oxidative stress. Bioorg. Med. Chem. Lett. 2014; 24:1344–8. [PubMed: 24508132]

de Gruijl FR. Photocarcinogenesis: UVA vs. UVB radiation. Skin Pharmacol. Physiol. 2002; 15:316–320.

Dickinson SE, Olson ER, Zhang J, Cooper SJ, Melton T, Criswell PJ, et al. P38 MAP kinase plays a functional role in UVB-induced mouse skin carcinogenesis. Mol. Carcinog. 2011; 50:469–478. [PubMed: 21268131]

Ding SZ, Yang YX, Li XL, Michelli-Rivera A, Han SY, Wang L, et al. Epithelial–mesenchymal transition during oncogenic transformation induced by hexavalent chromium involves reactive oxygen species-dependent mechanism in lung epithelial cells. Toxicol. Appl. Pharmacol. 2013; 269:61–71. [PubMed: 23518002]

Einspahr JG, Timothy BG, Alberts DS, McKenzie N, Saboda K, Warneke J, et al. Cross-validation of murine UV signal transduction pathways in human skin. Photochem. Photobiol. 2008; 84:463–476. [PubMed: 18248498]

Feng R, Bowman LL, Lu Y, Leonard SS, Shi X, Jiang BH, et al. Blackberry extracts inhibit activating protein 1 activation and cell transformation by perturbing the mitogenic signaling pathway. Nutr. Cancer. 2004; 50:80–89. [PubMed: 15572301]

Fischer SM, Pavone A, Mikulec C, Langenbach R, Rundhaug JE. Cyclooxygenase-2 expression is critical for chronic UV-induced murine skin carcinogenesis. Mol. Carcinog. 2007; 46:363–371. [PubMed: 17219415]

Gallo O, Fini-Storchi I, Vergari WA, Masini E, Morbidelli L, Ziche M, et al. Role of nitric oxide in angiogenesis and tumor progression in head and neck cancer. J. Natl. Cancer Inst. 1998; 90:587–596. [PubMed: 9554441]

Gu M, Singh RP, Dhanalakshmi S, Agarwal C, Agarwal R. Silibinin inhibits inflammatory and angiogenic attributes in photocarcinogenesis in SKH-1 hairless mice. Cancer Res. 2007; 67:3483–3491. [PubMed: 17409458]

Halvorsen BL, Carlsen MH, Phillips KM, Bøhn SK, Holte K, Jacobs DR, et al. Content of redox-active compounds (ie, antioxidants) in foods consumed in the united states. Am. J. Clin. Nutr. 2006; 84:95–135. [PubMed: 16825686]

Heck DE, Vetrano AM, Mariano TM, Laskin JD. UVB light stimulates production of reactive oxygen species unexpected role for catalase. J. Biol. Chem. 2003; 278:22432–22436. [PubMed: 12730222]

Author Manuscript Author Manuscript Author Manuscript Author Manuscript

Hsieh CL, Yen GC, Chen HY. Antioxidant activities of phenolic acids on ultraviolet radiation-induced erythrocyte and low density lipoprotein oxidation. J. Agric. Food Chem. 2005; 53:6151–6155. [PubMed: 16029010]

Khan N, Syed DN, Pal HC, Mukhtar H, Afaq F. Pomegranate fruit extract inhibits uvb-induced inflammation and proliferation by modulating NF-κB and mapk signaling pathways in mouse skin. Photochemistry and Photobiology. 2012; 88:1126–1134. [PubMed: 22181855]

Koh HK. Preventive strategies and research for ultraviolet-associated cancer. Environ. Health Perspect. 1995; 103:255. [PubMed: 8741794]

Lee CW, Ko HH, Chai CY, Chen WT, Lin CC, Yen FL. Effect of artocarpus communis extract on UVB irradiation-induced oxidative stress and inflammation in hairless mice. Intl. J. Mol. Sci. 2013; 14:3860–3873.

Lee JA, Jung BG, Kim TH, Lee SG, Park YS, Lee BJ. Dietary feeding of opuntia humifusa inhibits UVB radiation-induced carcinogenesis by reducing inflammation and proliferation in hairless mouse model. Photochem. Photobiol. 2013; 89:1208–1215. [PubMed: 23789636]

Mantena SK, Katiyar SK. Grape seed proanthocyanidins inhibit UV-radiation-induced oxidative stress and activation of MAPK and NF-κB signaling in human epidermal keratinocytes. Free Rad. Biol. Med. 2006; 40:1603–1614. [PubMed: 16632120]

Merwald H, Klosner G, Kokesch C, Der-Petrossian M, Hönigsmann H, Trautinger F. UVA-induced oxidative damage and cytotoxicity depend on the mode of exposure. J. Photochem. Photobiol. B: Biology. 2005; 79:197–207.

Murapa P, Dai J, Chung M, Mumper RJ, D'Orazio J. Anthocyanin-rich fractions of blackberry extracts reduce UV-induced free radicals and oxidative damage in keratinocytes. Phytother. Res. 2012; 26:106–112. [PubMed: 21567508]

Phillips J, Moore-Medlin T, Sonavane K, Ekshyyan O, McLarty J, Nathan C. Curcumin inhibits UV radiation–induced skin cancer in SKH-1 mice. Otolaryngol. Head Neck Surg. 2013; 148:797–803. [PubMed: 23386626]

Pratheeshkumar P, Kuttan G. Cardiospermum halicacabum inhibits cyclophosphamide induced immunosupression and oxidative stress in mice and also regulates iNOS and COX-2 gene expression in LPS stimulated macrophages. Asia. Pac. J. Cancer Prev. 2010; 11:1245–1252.

Pratheeshkumar P, Kuttan G. Modulation of immune response by vernonia cinerea l. Inhibits the proinflammatory cytokine profile, iNOS, and COX-2 expression in LPS-stimulated macrophages. Immunopharmacol. Immunotoxicol. 2011; 33:73–83. [PubMed: 20367552]

Pratheeshkumar P, Kuttan G. Vernolide-A, a sesquiterpene lactone from vernonia cinerea, induces apoptosis in B16F-10 melanoma cells by modulating p53 and caspase-3 gene expressions and regulating NF-κB-mediated Bcl-2 activation. Drug Chem. Toxicol. 2011; 34:261–270. [PubMed: 21649480]

Pratheeshkumar P, Sreekala C, Zhang Z, Budhraja A, Ding S, Son YO, et al. Cancer prevention with promising natural products: Mechanisms of action and molecular targets. AntiCancer Agents Med. Chem. 2012; 12:1159–1184. [PubMed: 22583402]

Pratheeshkumar P, Son YO, Wang X, Divya SP, Joseph B, Hitron JA, et al. Cyanidin-3-glucoside inhibits uvb-induced oxidative damage and inflammation by regulating MAP kinase and NF-κB signaling pathways in SKH-1 hairless mice skin. Toxicol. Appl. Pharmacol. 2014; 280:127–137. [PubMed: 25062774]

Robinson JK. Sun exposure, sun protection, and vitamin D. Jama. 2005; 294:1541–1543. [PubMed: 16193624]

Rogers HW, Weinstock MA, Harris AR, Hinckley MR, Feldman SR, Fleischer AB, et al. Incidence estimate of nonmelanoma skin cancer in the United States, 2006. Arch. Dermatol. 2010; 146:283–287. [PubMed: 20231499]

Sano Y, Park JM. Loss of epidermal p38α signaling prevents ultraviolet radiation-induced inflammation via acute and chronic mechanisms. J. Invest. Dermatol. 2014; 134:2231–40. [PubMed: 24662766]

Sarasin A. The molecular pathways of ultraviolet-induced carcinogenesis. Mutat. Res. 1999; 428:5–10. [PubMed: 10517972]

Author Manuscript Author Manuscript Author Manuscript Author Manuscript

Seeram NP, Adams LS, Zhang Y, Lee R, Sand D, Scheuller HS, et al. Blackberry, black raspberry, blueberry, cranberry, red raspberry, and strawberry extracts inhibit growth and stimulate apoptosis of human cancer cells in vitro. J. Agric. Food Chem. 2006; 54:9329–9339. [PubMed: 17147415]

Sharma SD, Meeran SM, Katiyar SK. Dietary grape seed proanthocyanidins inhibit UVB-induced oxidative stress and activation of mitogen-activated protein kinases and nuclear factor-κB signaling in in vivo SKH-1 hairless mice. Mol. Cancer Ther. 2007; 6:995–1005. [PubMed: 17363493]

Sharma SD, Katiyar SK. Dietary grape seed proanthocyanidins inhibit UVB-induced cyclooxygenase-2 expression and other inflammatory mediators in UVB-exposed skin and skin tumors of SKH-1 hairless mice. Pharm. Res. 2010; 27:1092–1102. [PubMed: 20143255]

Society, AC. Cancer facts & figures. 2012.

Sumiyoshi M, Kimura Y. Effects of a turmeric extract (Curcuma longa) on chronic ultraviolet B irradiation-induced skin damage in melanin-possessing hairless mice. Phytomedicine. 2009; 16:1137–1143. [PubMed: 19577913]

Vaid M, Sharma SD, Katiyar SK. Proanthocyanidins inhibit photocarcinogenesis through enhancement of DNA repair and xeroderma pigmentosum group A–dependent mechanism. Cancer Prev. Res. 2010; 3:1621–1629.

Vayalil PK, Elmets CA, Katiyar SK. Treatment of green tea polyphenols in hydrophilic cream prevents UVB-induced oxidation of lipids and proteins, depletion of antioxidant enzymes and phosphorylation of mapk proteins in SKH-1 hairless mouse skin. Carcinogenesis. 2003; 24:927–936. [PubMed: 12771038]

Wang QS, Xiang Y, Cui Y,L, Lin KM, Zhang XF. Dietary blue pigments derived from genipin, attenuate inflammation by inhibiting LPS-induced iNOS and COX-2 expression via the NF-κB inactivation. PLoS One. 2012; 7:e34122. [PubMed: 22479539]

Yin Y, Li W, Son YO, Sun L, Lu J, Kim D, et al. Quercitrin protects skin from UVB-induced oxidative damage. Toxicol. Appl. Pharm. 2013; 269:89–99.

Yoon JH, Lim TG, Lee KM, Jeon AJ, Kim SY, Lee KW. Tangeretin reduces ultraviolet B (UVB)-induced cyclooxygenase-2 expression in mouse epidermal cells by blocking mitogen-activated protein kinase (MAPK) activation and reactive oxygen species (ROS) generation. J. of Agric. Food Chem. 2010; 59:222–228. [PubMed: 21126077]

Yoshida E, Watanabe T, Takata J, Yamazaki A, Karube Y, Kobayashi S. Topical application of a novel, hydrophilic γ-tocopherol derivative reduces photo-inflammation in mice skin. J. Invest. Dermatol. 2006; 126:1633–1640. [PubMed: 16543897]

Zhaorigetu S, Yanaka N, Sasaki M, Watanabe H, Kato N. Inhibitory effects of silk protein, sericin on UVB-induced acute damage and tumor promotion by reducing oxidative stress in the skin of hairless mouse. J. Photochem. Photobiol. B: Biol. 2003; 71:11–17.

Author Manuscript Author Manuscript Author Manuscript Author Manuscript

Highlights

- Blackberry extract inhibits UVB-induced glutathione depletion.
- Blackberry extract inhibits UVB-induced lipid peroxidation.
- Blackberry extract inhibits UVB-induced myeloperoxidase activity.
- Blackberry extract diminishes UVB-induced inflammatory responses.
- Blackberry extract prevents skin from oxidative damage and inflammation by UVB.

Author Manuscript Author Manuscript Author Manuscript Author Manuscript

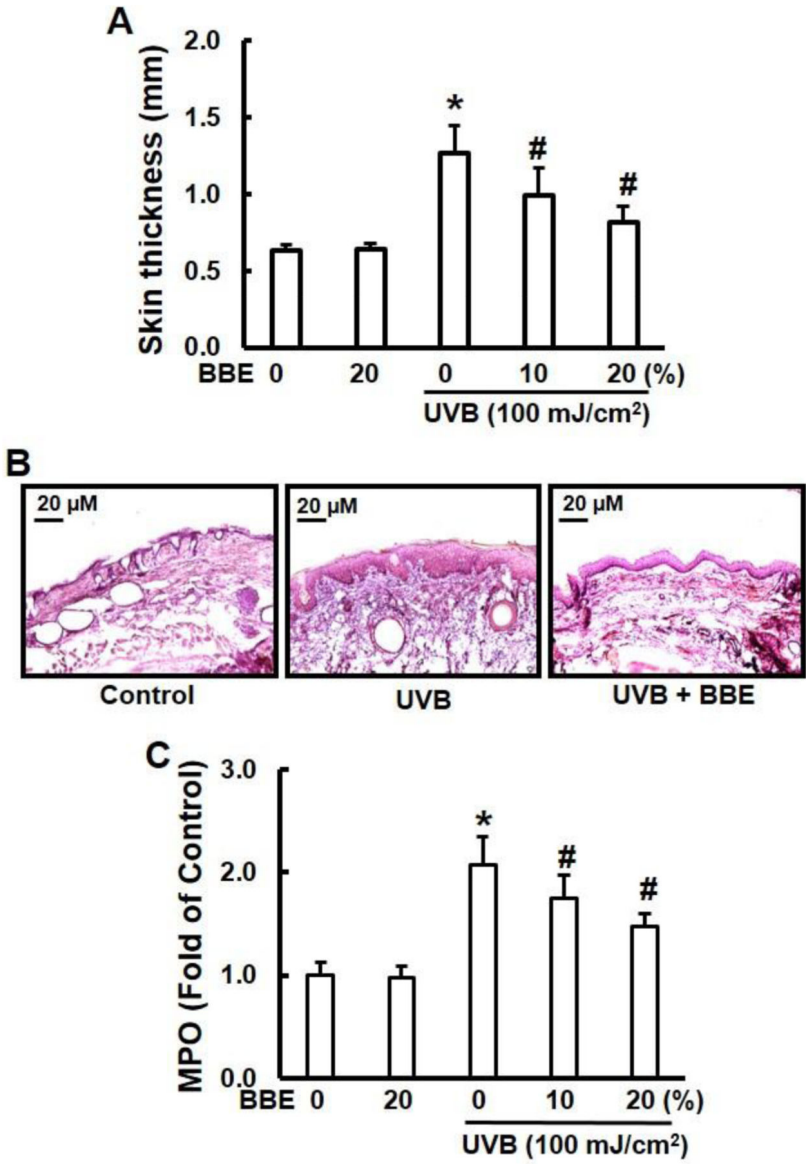

Fig. 1.

BBE inhibits UVB-induced skin edema. (A) BBE inhibits UVB-induced hyperplastic response in terms of the epidermal thickness (mm). The dorsal skin of female SKH-1 mice was UVB-irradiated (100 mJ/cm^2) three times a week for a total of 10 weeks. Topical treatments included either acetone (control group) or BBE (10% and 20% in acetone) one day prior to UVB exposure. Mice were sacrificed after 10 weeks of UVB irradiation; skin was collected and the thickness measured. (B) Representative photomicrographs of H&E staining of mouse skin **from groups of control, UVB, and UVB with 20% BBE.** (C) MPO was determined as a marker of UVB-induced cutaneous infiltration. Reported data are the fold change (n=6). * and #, $p<0.05$ compared to control without treatment and UVB treatment alone, respectively.

Author Manuscript Author Manuscript Author Manuscript Author Manuscript

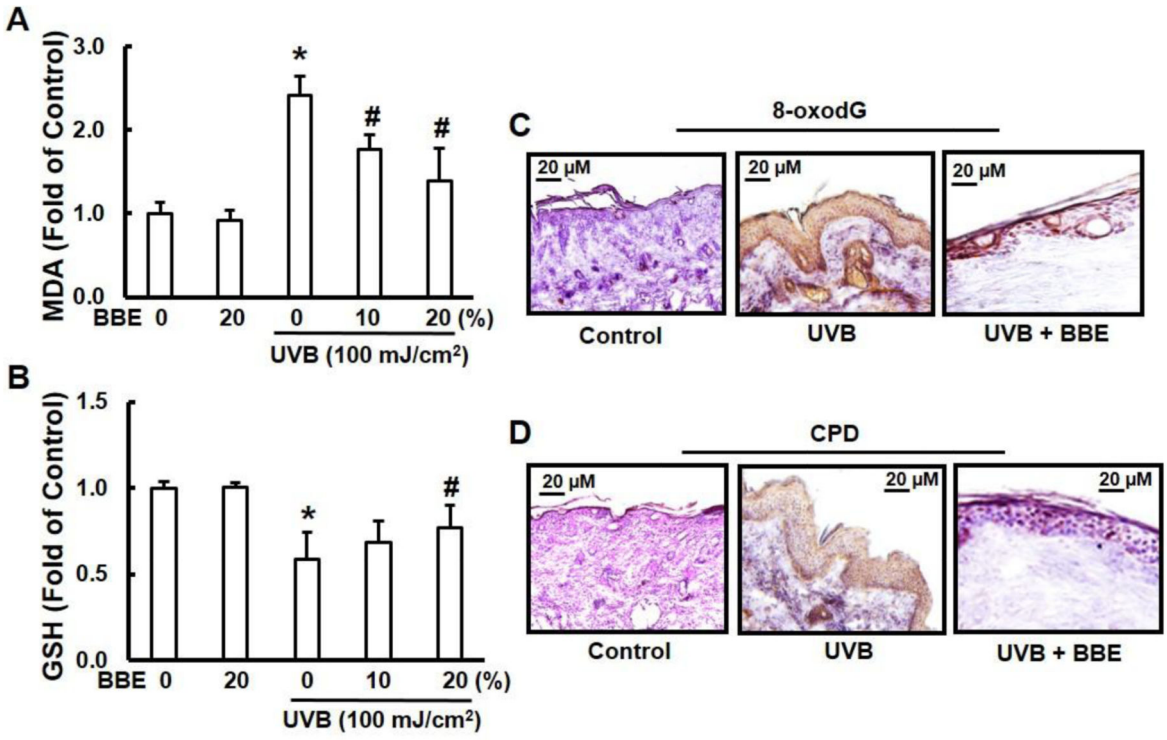

Fig. 2.

BBE inhibits UVB-induced oxidative stress and DNA damage in mouse skin. UVB irradiation and BBE treatment proceeded as described previously. Animals were sacrificed at the indicated time points. Skin samples were collected and homogenized by sonication in ice cold PBS. Tissue lysate was used for the determination of oxidative stress in terms of (A) lipid peroxidation and (B) glutathione depletion. * and #, $p<0.05$ compared to control without treatment and UVB treatment alone, respectively. (C) and (D) Mouse skin from groups of control, UVB, and UVB with 20% BBE was used for immunohistochemistry analysis. (C) **8-oxodG** formation. (D) Cyclobutane pyrimidine dimer formation. Immunoperoxidase staining for the antibodies is dark brown, and the photomicrographs are representative of three independent experiments with similar results.

Author Manuscript Author Manuscript Author Manuscript Author Manuscript

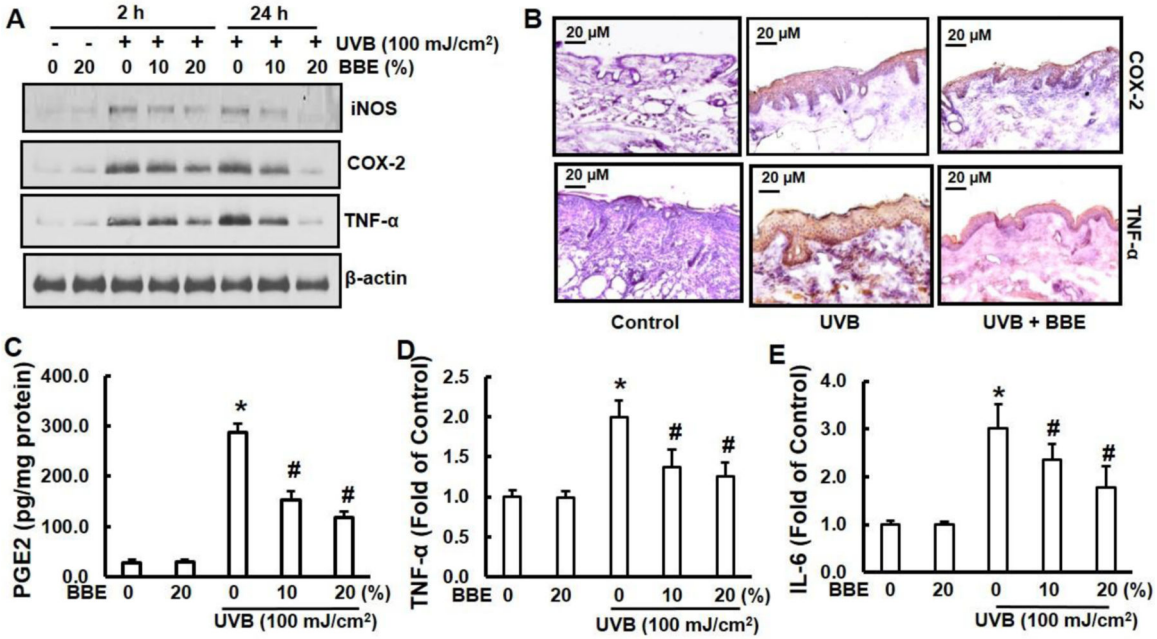

Fig. 3.

BBE inhibits UVB-induced COX-2, iNOS, PGE_2 and proinflammatory cytokines in mouse skin. UVB irradiation and BBE treatment proceeded as described previously. Animals were sacrificed at the indicated time points. Tissue lysates were prepared as described in the Methods section. (A) The protein expressions of COX-2, iNOS and TNF-α were determined in tissue lysates using Western blot analysis. The β-actin signal confirms equal loading of protein samples. (B) Frozen skin sections (5 μM thick) **from groups of control, UVB, and UVB with 20% BBE** were immunohistochemistry stained for COX-2 (1:100) and TNF-α (1:200) expression that is dark brown. (C) Epidermal PGE_2 was determined as a marker of inflammation as described in the Methods section. The concentration of PGE_2 is expressed as pg per mg protein, and data presented are a mean ± SD (n=6). The levels of proinflammatory cytokines TNF-α (D) and IL-6 (E) in tissue samples were determined using cytokine-specific ELISA following the manufacturer's protocol. * and #, $p<0.05$ compared to control without treatment and UVB treatment alone, respectively.

Author Manuscript Author Manuscript Author Manuscript Author Manuscript

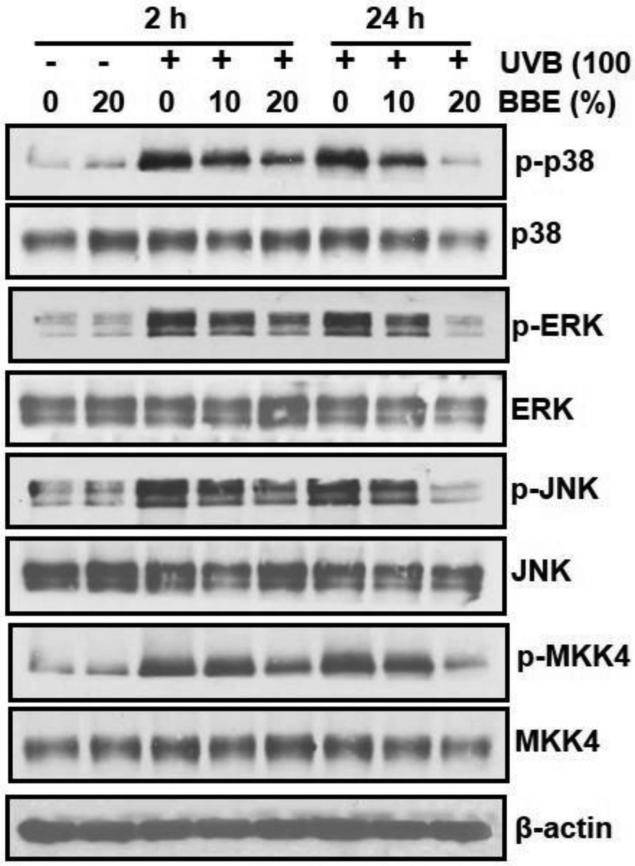

Fig. 4.

BBE inhibits UVB-induced MAPK signalling in mouse skin. UVB irradiation and BBE treatment proceeded as described previously. Animals were sacrificed at 2 h and 24 h after 10 weeks of UVB irradiation, and tissue lysates were prepared to determine the total and phosphorylated protein levels of ERK1/2, p38, JNK and MKK4 using immunoblotting analysis, as described in the Methods section. A representative blot from three independent experiments with identical results is shown.

Author Manuscript Author Manuscript Author Manuscript Author Manuscript

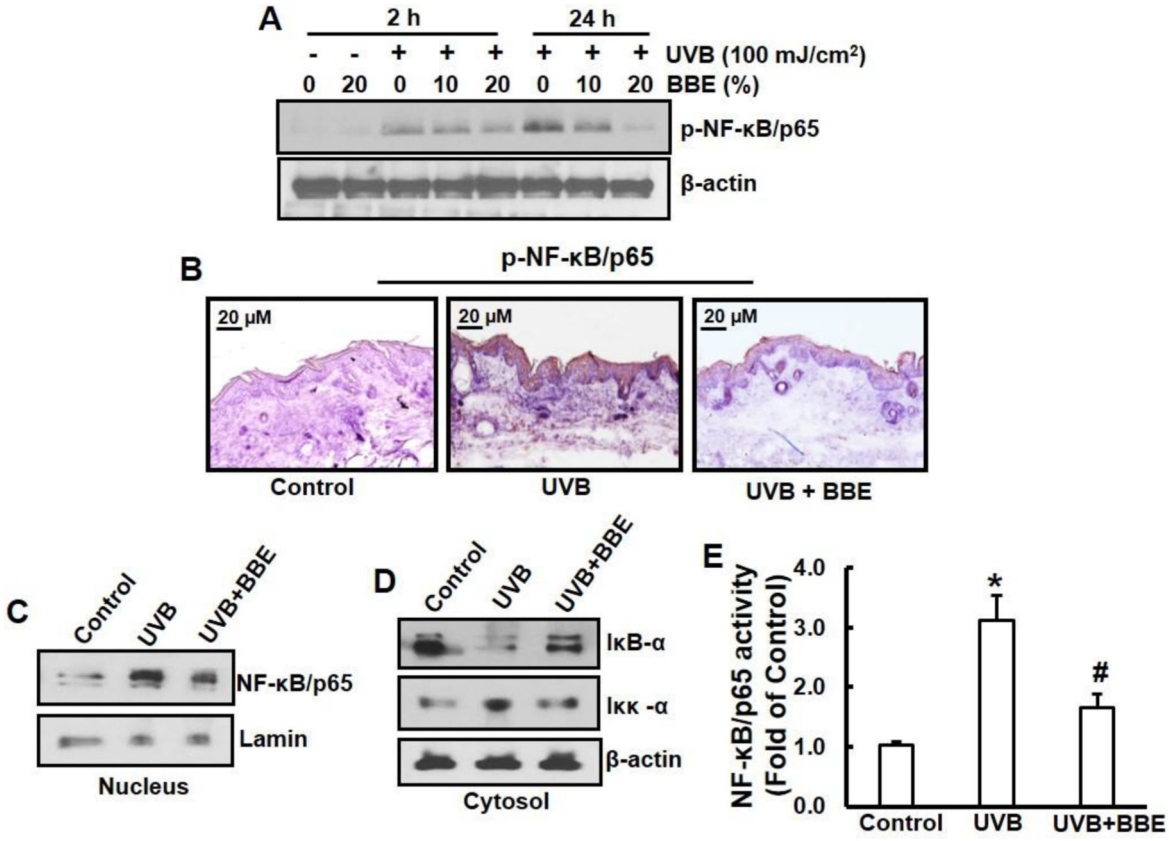

Fig. 5.

BBE inhibits UVB-induced activation of NF-κB/p65 and IKKα, and degradation of IκBα in mouse skin. UVB irradiation and BBE treatment proceeded as described previously. Animals were sacrificed at 2 h and 24 h after 10 weeks of UVB irradiation, and tissue lysates were prepared. (A) Immunoblotting analysis for the phosphorylation/activation of NF-κB/p65. (B) Immunohistochemistry staining for pNF-κB/p65 expression in the mouse skin from groups of control, UVB, and UVB with 20% BBE. (C) Immunoblotting analysis for nuclear translocation of NF-κB/p65. (D) Immunoblotting analysis for activation of IKKα, or degradation of IκBα in cytosol. For each analysis, a representative blot from three independent experiments with identical observations is shown, and equivalent protein loading was confirmed by probing stripped blots for β-actin. (E) The activity of NF-κB in nuclear fraction of skin lysates is presented. * and #, $p<0.05$ compared to control without treatment and UVB treatment alone, respectively.

Author Manuscript Author Manuscript Author Manuscript Author Manuscript

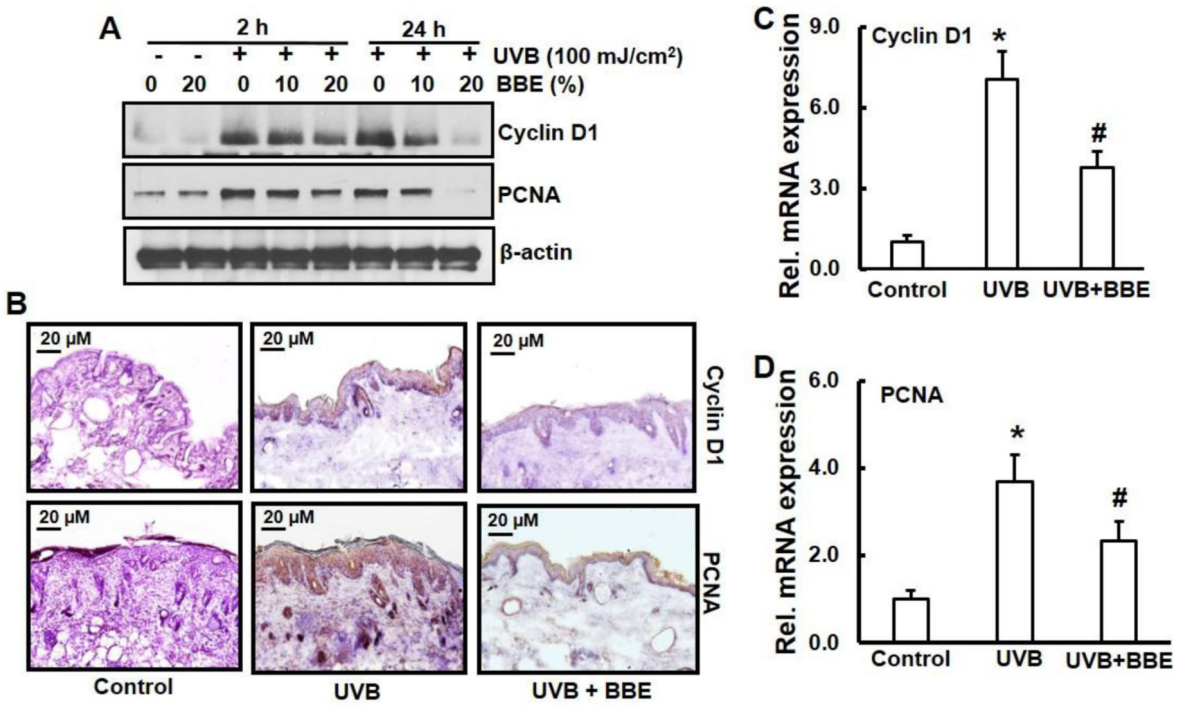

Fig. 6.

BBE inhibits UVB induced cell proliferation marker, cyclin-D1 and PCNA in mouse skin. UVB irradiation and BBE treatment proceeded as described previously. Animals were sacrificed at 2 h and 24 h after 10 weeks of UVB irradiation, and tissue lysates were prepared. The levels of cyclin-D1 and PCNA in mouse skin repeatedly exposed to UVB were detected by (A) Immunoblotting (B) Immunohistochemistry staining and (C-D) real time PCR as described in the Methods section. (B), (C), and (D), mouse skin samples are from groups of control, UVB, and UVB with 20% BBE. Presented data are the relative intensities of each band after normalization for the levels of β-actin. * and #, $p<0.05$ compared to control without treatment and UVB treatment alone, respectively.